Langmuir

Article

pubs.acs.org/Langmuir

Surface Tension-Induced Gel Fracture. Part 1. Fracture of Agar Gels

Constantinos Spandagos,[†] Thomas B. Goudoulas,[‡] Paul F. Luckham,[†] and Omar K. Matar*,[†]

[†]Department of Chemical Engineering & Chemical Technology, Imperial College of Science, Technology & Medicine, London SW7 2AZ

[‡]Department of Chemical Engineering, Aristotle University of Thessaloniki, Greece

Supporting Information

ABSTRACT: This work involves an experimental investigation of the spreading of liquids on gel layers in the presence of surfactants. Of primary interest is the instability that accompanies the cracking of gels through the deposition and subsequent spreading of a drop of surfactant solution on their surfaces. This instability manifests itself via the shaping of crack-like spreading "arms", in formations that resemble starbursts. The main aim of this study is to elucidate the complex interactions between spreading surfactants and underlying gels and to achieve a fundamental understanding of the mechanism behind the observed phenomenon of the cracking pattern formation. By spreading SDS and Silwet L-77 surfactant solutions on the surfaces of agar gels, the different ways that system parameters such as the surfactant chemistry and concentration and the gel strength can affect the morphology and dynamics of the starburst patterns are explored. The crack propagation dynamics is fitted to a power law by measuring the temporal evolution of the length of the spreading arms that form each one of the observed patterns. The values of the exponent of the power law are within the predicted limits for Marangoni-driven spreading on thick layers. Therefore, Marangoni stresses, induced by surface tension gradients between the spreading surfactant and the underlying gel layer, are identified to be the main driving force behind these phenomena, whereas gravitational forces were also found to play an important role. A mechanism that involves the "unzipping" of the gel in a manner perpendicular to the direction of the largest surface tension gradient is proposed. This mechanism highlights the important role of the width of the arms in the process; it is demonstrated that a cracking pattern is formed only within the experimental conditions that allow $S/\Delta w$ to be greater than G', where S is the spreading coefficient, Δw is the change in the width of the crack, and G' is the storage modulus of the substrate.

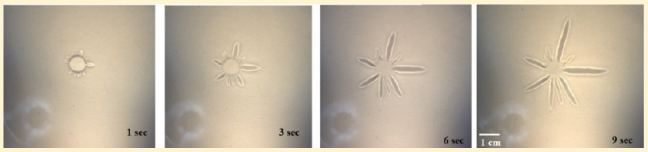

1. INTRODUCTION

The spreading of fluids over various substrates has attracted interest in many fields of science and technology such as environmental engineering, biomedicine, and the chemical and petrochemical industries.[1,2] The addition of surface-active agents (surfactants) can have a tremendous effect on the rate and extent of the spreading process. Therefore, the ability to control these properties can be beneficial in many applications, including surfactant replacement therapy,[3,4] lipid tear layers in the eye,[5] coating processes,[6] and the spraying of pesticides,[7] among others. That is the reason that surfactant-enhanced spreading has been investigated in numerous experimental and theoretical studies and has been the subject of two major reviews by Lee et al.[8] and Matar and Craster.[9] Such spreading processes have been shown to be accompanied by rich, interesting dynamics that owes its existence to the delicate interplay between the different mechanisms that play a role in the observed phenomena. These forces are operative over a large range of scales, complicating the understanding of the relative contribution of each one of them, the derivation of appropriate predictive models, and the performance of simulations of the spreading process.

Although the spreading of thin films on liquids and rigid solids has been the subject of numerous studies, the majority of these studies have largely focused on the case of Newtonian fluids and materials having relatively simple rheology (an elastic, rigid solid or another Newtonian liquid, for instance). The dynamics of spreading on compliant substrates of complex rheology, however, has received less attention in the literature. A limited number of studies on the spreading on gel-like materials have been carried out[10,11] and very few of these feature the spreading of surfactant-laden liquids. This is particularly surprising given the scientific and industrial interest that the nature of a gel-like material can have because it is possible to exhibit the full spectrum of solid-like to liquid-like behavior simply by changing the gel concentration. Furthermore, the complex interactions between spreading liquids and underlying gel-like materials are a problem that lies at the heart of a wide range of engineering, biological, biomedical, and daily life applications, which include drug delivery over compliant substrates such as the spreading of bioadhesive or mucoadhesive liquids over tissue,[12] or over mucus-laden films[13] in the lung,[14] or elsewhere in the body; the development of scaffolds in tissue engineering, which are porous, degradable structures that can be gels, designed to degrade within the patient[15] (however, it is sometimes required that drugs are administered through or over the scaffold without fracturing it). Understanding and improving the emplacement, fracturing, and

Received: December 31, 2011
Revised: April 11, 2012
Published: April 18, 2012

Table 1. Surface Tension Values of the Different SDS and Silwet L-77 Solutions Used in This Study

	concentration (cmc)					
SDS	0.4	0.8	1.2	2	2.8	4
surface tension (mN/m)	60 ± 0.5	52 ± 0.5	40.5 ± 0.5	35.5 ± 0.5	34.5 ± 0.5	33 ± 0.5
	concentration (cmc)					
Silwet L-77	0.6	1	2	4	6	8
surface tension (mN/m)	28 ± 0.5	25 ± 0.5	23 ± 0.5	22 ± 0.5	21 ± 0.5	20 ± 0.5

subsequent removal of gels in reservoirs in the oil industry, which is a commonly used technique[16,17] to limit water production while retaining oil or gas production; optimizing the deposition of multilayers of gel-like materials in the manufacturing of photographic films; and the spreading and subsequent breakup of particle rafts by surfactant,[18] which is relevant to the collapse of particle shells encapsulating drugs for inhalation delivery.[19]

It is expected that the interactions of the spreading liquid with the underlying gel-like material will lead to exceedingly complicated flow structures. This has been confirmed in a recent study by Daniels et al.[20,21] that has shown that such systems can also exhibit flow instabilities and complex behavior that are very poorly understood. This work considers the spreading of either pure silicon oil droplets, or droplets of Triton X-305 dissolved in deionized water on agar gels. These investigators report that the droplets are observed to spread into spreading arm patterns in formations that resemble a starburst.

The formation of these patterns can be considered to be behavior similar to the fingering instability that occurs on the surfaces of liquids and solids and has been reported in many experimental[22−35] and theoretical[36−46] studies, being mainly associated with the presence and spreading of surfactants. An example of the complex dynamics accompanying the spreading of a surfactant-laden droplet on a thin liquid film is provided by the work of Edmonstone et al.[47] in which it was demonstrated how the presence of surfactants at concentrations beyond the critical micelle concentration gives rise to a fingering instability that exhibits highly nonlinear processes such as tip splitting, merging, and shielding. The isolation of the mechanism underlying these patterns has been a hotly disputed topic in the literature since these patterns were reported for the first time.[22]

According to Daniels et al.,[21] the formation of the cracking patterns on the surfaces of gel layers is associated with the Marangoni effect;[48−50] however, a fundamental understanding of this new class of flow behavior has not yet been achieved, and the precise mechanism behind the intriguing observation of these patterns remains unclear. By experimentally examining important system parameters that can influence the instability, possible explanations can be investigated. Furthermore, it is possible that important contributions to the problem can be made by the use of a specific class of surfactants that have the unique ability to reduce the surface tension of water drastically and thus promote strikingly rapid spreading on very hydrophobic substrates, even in very small quantities.[51] These surfactants are termed superspreaders, and the phenomenon is called superspreading.[52−62] Recently, a mechanism for superspreading was proposed by Karapetsas et al.[63] whereby surfactant adsorption at the contact line was demonstrated to be primarily responsible for the rapid spreading observed for superspreaders. The contact line adsorption provides a mechanism for the removal of surfactant from the contact line region and an impetus for sustained Marangoni-driven spreading.

This work is aimed at achieving a fundamental understanding of this new class of flows that can be observed during the spreading of surfactants on the surfaces of gel layers. Through direct experimentation, the spreading of an anionic surfactant (SDS) and a nonionic trisiloxane (Silwet L-77) on thick underlying agar gel layers has been studied in order to provide insight into the nature of the liquid−gel interactions and examine the effect of varying important system parameters such as the gel and surfactant concentrations on the observed pattern characteristics and spreading dynamics. Furthermore, this work represents the first attempt to take into consideration the presence of superspreading surfactants in the cracking and pattern-forming process. A detailed rheological characterization of agar gels of various concentrations is aimed at identifying the link between the different experimental findings and the rheology of the underlying substrates.

2. EXPERIMENTAL DETAILS

2.1. Materials. The surfactants used in this study were anionic SDS (sodium dodecyl sulfate from Sigma-Aldrich U.K.) and nonionic Silwet L-77 (poly(alkyleneoxide)-modified heptamethyltrisiloxane 85% from De Sangosse U.K.). The choice of SDS is dictated by the fact that it has well- characterized properties[64,65] and is one of the most common materials used in studies on surfactants.[24,25,34,66−70] Its critical micelle concentration (cmc) is 2307 mg/L,[64] and its surface diffusivity, D_s, is on the order of 10^{-10} m^2/s.[65]

Silwet L-77 is a well-known superspreader. Superspreaders are surfactants that are able to reduce the surface tension of water drastically and promote rapid spreading on very hydrophobic substrates even in very small quantities. The surface diffusivity of Silwet L-77 was assumed to be of the same order of magnitude as the corresponding values for superspreading trisiloxane surfactants of similar molecular structure, also on the order of 10^{-10} m^2/s.[71] Its cmc was found to be ∼150 ± 16 mg/L at 20 °C. The latter, together with the surface tensions of all of the solutions, were measured using a platinum Wilhelmy plate suspended from a Krüss microbalance (model K10 automatic tensiometer from Krüss USA). Table 1 summarizes the surface tension values of the different SDS and Silwet L-77 solutions used in this study.

The underlying substrates consisted of agar, a polymer made from subunits of galactose, and one of the most extensively studied and used polysaccharides.[72,73] Agar gels are tunable gels because they can behave either as viscoelastic solids, or as liquids, depending on the concentration of their solutions.

2.2. Experimental Procedure and Visualization Technique. The water used to clean the glassware and prepare solutions was deionized and passed through a water purification unit comprising three cartridges: reverse osmosis, ion exchanger, and activated carbon (Barnstead Nanopure Systems U.K.). The purified water had a resistivity of 18 MΩ cm and a surface tension of 72.2 ± 0.5 mN/m at 23 °C.

Gel solutions were prepared by mixing agar powder (from Sigma Aldrich U.K.) with deionized water and heating the subsequent mixture. After heating, the mixtures were poured into 14-cm-diameter

dx.doi.org/10.1021/la205163n | Langmuir 2012, 28, 7197−7211

glass Petri dishes and allowed to set overnight. The resulting gel layers have a thickness of approximately 4 mm.

The spreading was visualized using shadowgraphy[74] in a setup that has similarities to that used by Daniels et al.[21] and enjoys the benefit of geometrical simplicity. The circular Petri dish containing agar gel layers of different concentrations was positioned on a flat surface above a paper screen. A Dino X-Lite digital microcamera with a 1.3 megapixel resolution and a magnification capability of up to 500× (model AM-413M, from Dino-Lite Europe) was used to record the spreading at a rate of 30 frames/s. To make the spreading patterns visible, because both the gels and the surfactant droplets were transparent, the Petri dish was illuminated using extra light from a white light fiber-optic lamp at maximum intensity (model KL 1500 LCD, from Schott U.K.). The latter was held at a slight angle above the Petri dish and moved around until optimal shadows of the spreading patterns were projected on the paper screen. A schematic sketch of the experimental setup is shown in Figure 1.

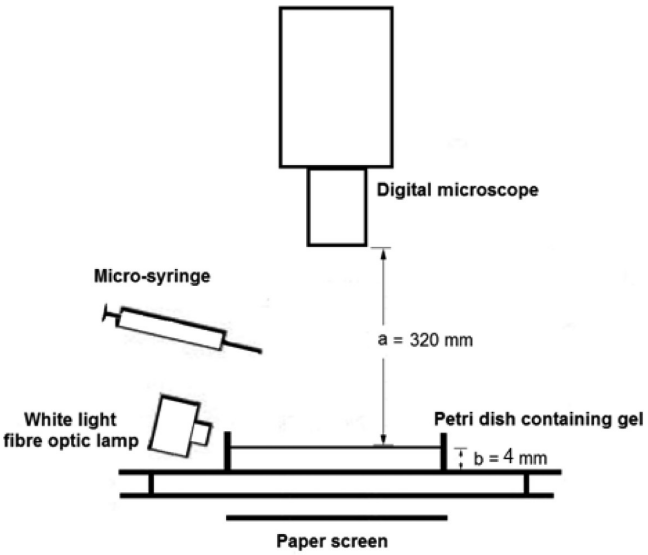

Figure 1. Schematic sketch of the experimental setup.

A 5 μL drop of surfactant solution of known concentration was delivered to the surface of the gel using a 20 μL precision microsyringe (from Hamilton U.K.). The drop was first released and allowed to hang from the tip of the needle and then to contact the surface of the gel layer in order to spread. This was done so as to minimize any effects that the dropping velocity would have on the gel fracture process. The spreading was followed for some seconds after deposition and recorded by the digital microscope. Each spreading run was repeated multiple times to ensure good reproducibility, and all of the experiments were conducted at ambient temperature and humidity.

2.3. Rheological Characterization of Agar Gel Solutions. The rheological properties of the agar gel solutions used in this study were measured by running the appropriate tests on an AR-G2 rheometer (from TA Instruments USA). This rheometer allows the characterization of sensitive samples because it has a magnetic thrust bearing that applies ultralow torques to the samples. A Peltier system on the lower place of the rheometer where the gel samples were placed allowed the temperature to be controlled to an accuracy of ±0.1 °C. Parallel plate geometry was used, having a titanium rotating disk of 40 mm diameter whereas the gap was up to 1150 μm, depending on the quantities and the response waveform of the gel sample. For the oscillatory measurements, the default value limits of the rheometer were 10^{-5} rad for the displacement and 5 μN m for the torque, and the tolerance within the measurement was 5% for the displacement and 1% for the torque. The software for the apparatus could depict the applied and measured waveforms for each final point of every oscillatory measurement so that it could be easily seen whether the results were in phase, or out of phase. It was also able to provide additional information by showing the 64 points consisting of each of the final waveforms.

Special care was taken with the loading of the samples in order to prevent the destruction of the structure of the gels due to shear movements and normal forces. The first sample for each concentration was effectively created on the lower plate of the rheometer (the Peltier base) by pouring the prepared solution into a polypropylene ring having the same diameter as the rotating disk. A closed plastic cylindrical cover was used to avoid evaporation and remained there for over 5 h. Then the ring was slowly removed, and gradually the titanium upper disk squashed the sample with steps of about 10 μm to a gap of 1000 μm, where good waveforms were observed during preliminary tests. After the procedure of setting the gap, the sample at the fixed gap was left to rest for at least 3 h and was covered again with the cylindrical cover. When rheological measurements on a sample from a previous batch were needed, (after 48 h, for instance), then the sample preparation was as follows: the glass pot containing the gel was slowly tilted to obtain the sample from the gel batch almost tangentially, rather than vertically, so that a slice of gel was obtained without any cracks in the structure and placed in the plate of the rheometer. The disk over the sample was slowly lowered, an adequate gap was fixed as previously described, and any overfill was removed gradually with a spatula. The same procedure as in the case of the first sample was repeated afterward.

After the preparation process described above, rheological measurements were conducted with oscillatory and steady-state flow conditions. Oscillatory measurements were performed at 20 °C to record the evolution of the mechanical properties in time, namely, G', G'', and η' against time, after the gelation of agar solutions. At the selected time intervals, typical frequency and temperature sweeps were also performed. Preliminary oscillatory time sweep measurements on agar samples at concentrations of 0.06 and 0.12 wt % during a period of 72 h showed that 10−12 h after preparation a stable response was achieved because practically constant values of G' and G'' with an increase of no more than 10% were obtained. By applying strain values of up to 0.4%, it was observed that the storage modulus G' was about an order of magnitude higher than the loss modulus G'' for applied frequencies of 0.06 to 10 rad/s, notably retaining both values in time, even after 96 h in certain cases.

Representative results for the storage modulus G' and loss modulus G'' of agar gel solutions of varying concentrations over time sweeps are shown in Figure 2a,b, respectively. It should be noted that in all cases the raw phase difference between the application and the response of the gels was between 3.5 and 5.5 degrees, indicating almost purely elastic behavior even for the lower weight percent agar gels.

The experiments were performed at the same frequency of 0.5 Hz (3.14 rad/s) except for the 0.08 wt % agar, where this frequency was close to the nonlinear region. This concentration seems to have a narrow linear viscoelastic region, and low frequencies are needed to give relatively smooth waveforms (i.e., after the 0.5 Hz distorted waveform was recorded), so a frequency of 0.04 Hz was chosen for the time sweeps. As shown in Figure 2, the storage modulus is constant over wide period of measuring time (over an hour), and the loss modulus appears to be more sensitive in time, showing some fluctuation, mainly for lower agar concentrations. From these data, Figure 3, which summarizes the concentration effect on the storage modulus G' and loss modulus G'', is formed.

The data in Figure 3 indicate that there is a semilogarithmic correlation of the mechanical properties with the weight percent agar concentration, whereas the elastic character of the material is dominant (i.e., $\tan\delta \ll 1$, where $\tan\delta = G''/G'$) throughout the investigated concentration range.

3. RESULTS

3.1. Spreading of SDS. The spreading of droplets of aqueous SDS solution over a range of surfactant concentrations on agar gel layers of varying concentrations and strengths yields three types of qualitatively different regimes: the droplet remains approximately circular at the point of deposition;

dx.doi.org/10.1021/la205163n | Langmuir 2012, 28, 7197−7211

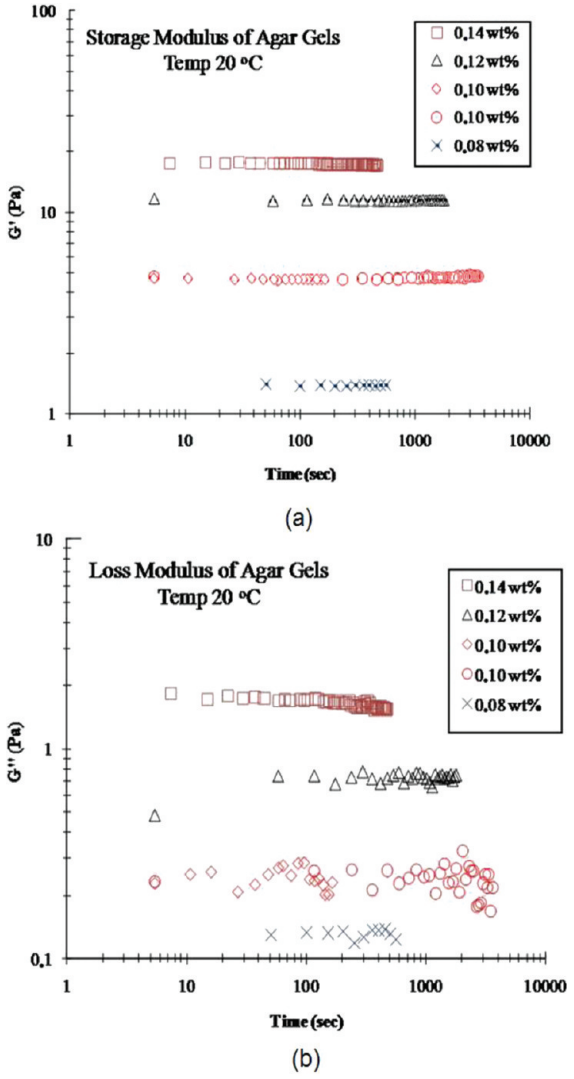

Figure 2. Time sweeps for agar gels of concentrations from 0.08 to 0.14 wt % for (a) the storage modulus and (b) the loss modulus. The frequency was 3.14 rad/s, except for a concentration 0.08 wt %, where it was 0.25 rad/s.

cracking patterns develop ahead of the deposition point; or the droplet spreads out, as it would on a liquid substrate, with no pattern formation. It is evident that the starburst pattern formation occurs only under intermediate conditions, when the concentration of the gel allows it to have elements from both solid-like and liquid-like behaviors. A summary of the observed behavior corresponding to the experimental conditions investigated in this study is given in Figure 4.

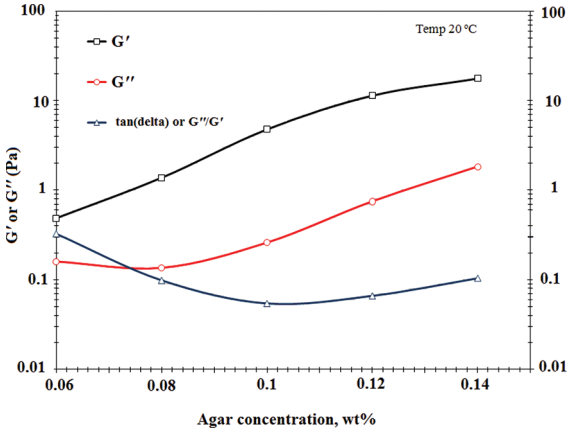

Figure 3. Effect of the weight percent agar concentration on G' and G''.

All of the cracking patterns observed here seem to have a central darker region that is surrounded by a brighter border. The latter represents the contact line between the crack and the uncontaminated gel. This indicates that the crack has a depth and it penetrates into the surface of the gel and that the region between the crack and the uncontaminated gel surface is slightly elevated.

An increase in the surfactant concentration up to and around the SDS cmc results mainly in the development of a flow instability that is much more evident than in the case of lower SDS concentrations. Above the cmc, there is a clear formation of patterns with visible, well-defined crack arms for all cases investigated between gel concentrations of 0.06 and 0.12 wt %. Immediately after deposition, these arms are observed to grow from the point of the drop deposition region and to extend further into the surfactant-free regions of the gel surface. The arms are mostly straight, with some exceptions observed in the patterns formed from 0.8 to 1.2 cmc and from 4 cmc drops (Figure 5B,F) and also in the patterns seen in the weakest gel of 0.06 wt % concentration (e.g., Figure 5E). On weaker gels (concentrations from 0.06 to 0.08 wt %), the arms are noticeably longer and narrower. On intermediate gels (from 0.08 to 0.12 wt %), the arms are generally smaller in size. When highly concentrated surfactant droplets are used, numerous long arms can be seen (Figure 5F). No clearly visible arms can be observed at gel concentrations of 0.14 wt % and above, with the single exception being the arm that is observed for a highly concentrated drop of 4 cmc. Thus, this is the upper limit of the flow instability for SDS. On much weaker gels and for concentrations near 0.04 wt % and below, the drops spread out as they would on a liquid substrate, and the formation of fingering patterns similar to those reported during the spreading of SDS on thin liquid films is observed.[34]

Figure 6 shows a typical example of the spatiotemporal evolution of the crack-like patterns. The arms start to grow from the region of drop deposition that seems to be like a circular disk, and they propagate along the surface of the gel. Most patterns observed here have been developed fully after a time of approximately 30 s.

During typical spreading processes of liquids, either on other liquids, or on solids, the spreading front advances with time following a power law of the following form

$$L(t) \approx kt^n \tag{1}$$

where $L(t)$ denotes the radial extent of spreading, k is a prefactor, t is the spreading time, and n is the spreading exponent; the latter provides an indication of the balance between the dominant forces involved in the spreading phenomena.[75] In this study, the spreading fronts are clearly nonaxisymmetric with spreading arms being formed instead. Therefore, a uniform spreading front and a radial extent of spreading cannot be described; what is important instead is the length of the spreading arms and how this changes with time. Hence, in the power law described by eq 1, L will denote the length of a spreading arm for the remainder of this article. To determine the spreading exponent n, the same method used by Daniels et al.[21] was employed; values of the spreading exponent of each one of the arms of a single pattern were obtained from

dx.doi.org/10.1021/la205163n | Langmuir 2012, 28, 7197–7211

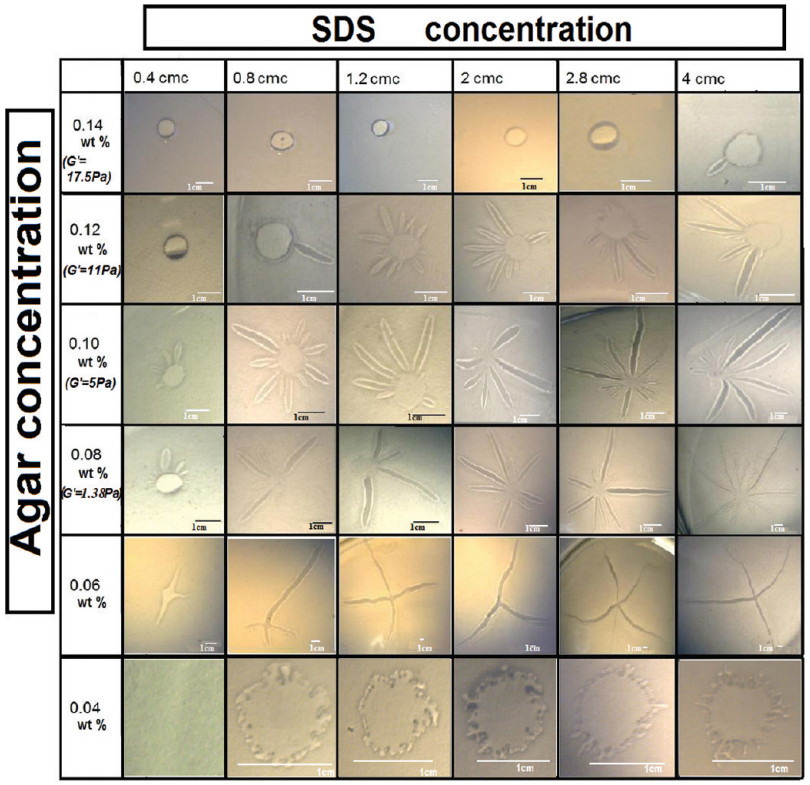

Figure 4. Pattern map showing fully developed patterns from SDS droplets of different concentrations that have spread on approximately 4-mm-thick agar gel layers of varying concentrations.

logarithmic plots of the evolution of its length for approximately the same time duration in each case. From such plots, both n and k were determined. Each arm of the same pattern was found to have a somewhat different spreading exponent value; these were then ensemble-averaged for the experimental runs associated with a surfactant and a gel concentration pairing in order to find a single spreading exponent value for each pattern. The results are shown in Figure 7.

The majority of the values of n were found to be very close to $^3/_4$ and are independent of gel and surfactant concentrations. Therefore, there seems to be a broad agreement with the $t^{3/4}$ scaling prediction, which is characteristic of the Marangoni-driven spreading of a finite mass of surfactants on thick films, suggesting that Marangoni stresses are dominant.[2,76,77]

To determine the spreading rate, or the velocity of the evolution of the spreading arms, we consider the following: Differentiating eq 1 gives

$$\frac{dL}{dt} = nkt^{n-1} \tag{2}$$

where dL/dt denotes the growth velocity of an arm. Fitting $n = {}^3/_4$ in eq 2 gives

$$\frac{dL}{dt} = \frac{3}{4}kt^{-1/4} \tag{3}$$

dL/dt is proportional to power-law prefactor k; therefore, k can be used to describe the spreading velocity. The higher the value of k, the higher the velocity.

The general trend discerned from Figure 8, which summarizes the different values of log k found for different values of log G' and for different SDS concentrations, is that k has higher values for weaker gels (lower G') and lower values for stronger gels (higher G'), thus it is suggested that the faster evolution of cracks occurs on the surfaces of weaker gels whereas slower evolution occurs on stronger gels. It seems that the driving force for cracking is more favorable to overcoming the retarding effects of gel rheology in cases where the gel is weak. An increase in the concentration (strength) of the gel increases the resistance of its rigidity against the force that promotes the propagation of the crack, resulting in smaller spreading rates. For a fixed gel concentration, there seems to be a tendency for increasing SDS concentration to increase k; however, this is mostly the case for surfactant concentrations up to 2 cmc.

Increasing the concentration of the gel seems to have an effect on the width of the arms, with the latter being thinner as the gel becomes stronger. This behavior is illustrated in Figure 9, where the storage modulus is again a measure of the gel concentration (strength).

3.2. Spreading of Silwet L-77. The spreading of drops of aqueous Silwet L-77 solution over a range of surfactant and gel concentrations gives rise to a range of behaviors broadly similar to those observed in the spreading of SDS. The main difference is the fact that the starburst patterns can now be formed over wider ranges of gel and surfactant concentrations (Figure 10).

The presence of Silwet L-77 can make it possible for these formations to occur on the surfaces of gels with concentrations of around 0.14 wt % at one extreme, or even on the surfaces of gels with concentrations of around 0.04 wt % at the other extreme, something that was not observed in the case of SDS. In addition, droplets of SDS of very low concentrations (below 0.4 cmc) produce no visible arms, whereas Silwet L-77 droplets of lower concentrations can still generate cracks, which, although shallow and small, are nevertheless still visible.

dx.doi.org/10.1021/la205163n | Langmuir 2012, 28, 7197−7211

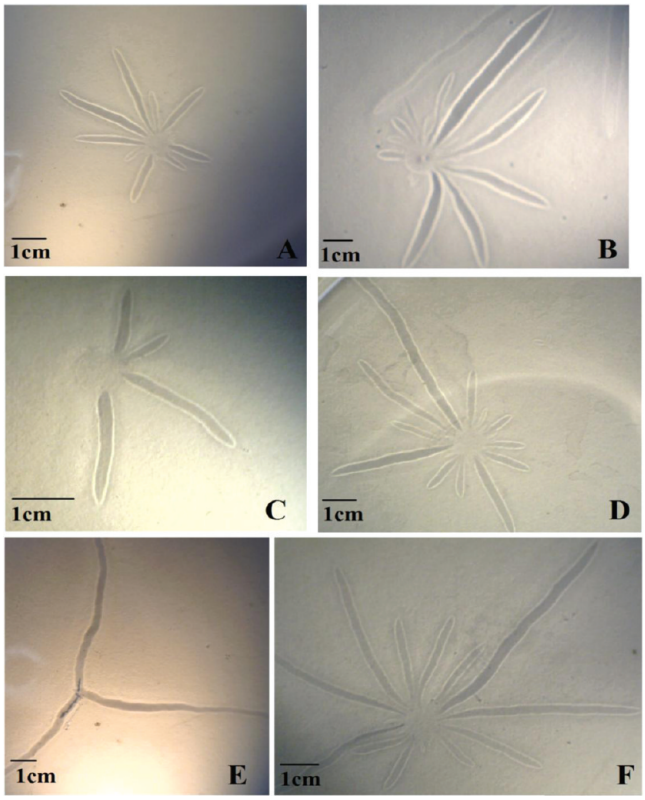

Figure 5. Close-up view of shadowgraph images of fully developed patterns after the spreading of (A) 2 cmc SDS on 0.08 wt % agar, (B) 4 cmc SDS on 0.10 wt % agar, (C) 1.2 cmc SDS on 0.08 wt % agar, (D) 2.8 cmc SDS on 0.10 wt % agar, (E) 2 cmc SDS on 0.06 wt % agar, and (F) 4 cmc SDS on 0.08 wt % agar.

It is also important that in most of cases, and mostly for agar concentrations lower than 0.10 wt %, the cracks start to form and propagate directly from the spot where the deposited

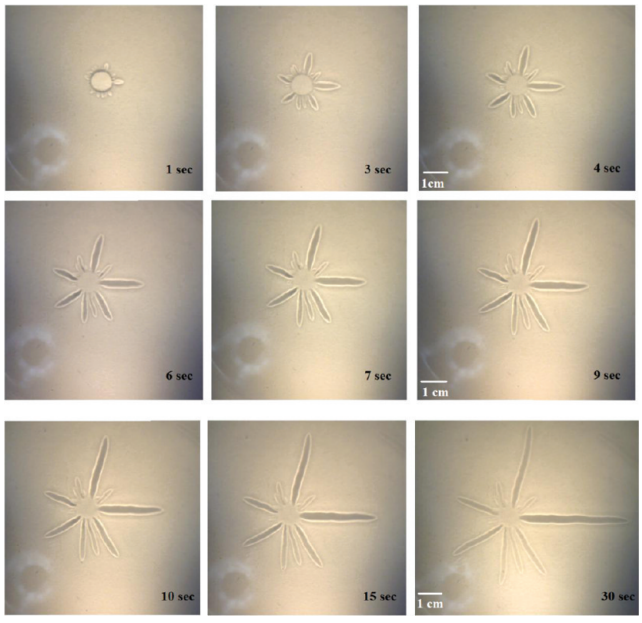

Figure 6. Spreading pattern evolution with time after the deposition of a 2.8 cmc SDS droplet on a 0.08 wt % agar gel. After t = 30 s, the evolution is complete.

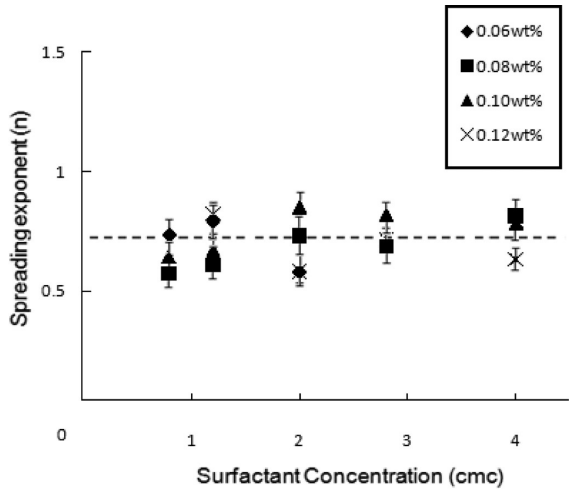

Figure 7. Variation of the spreading exponent with SDS concentration for spreading on agar gel layers of different agar concentrations. These points represent the average of multiple runs. The dashed line is the theoretical value of $^3/_4$, which is characteristic of Marangoni-driven spreading on thick layers.[2,76,77]

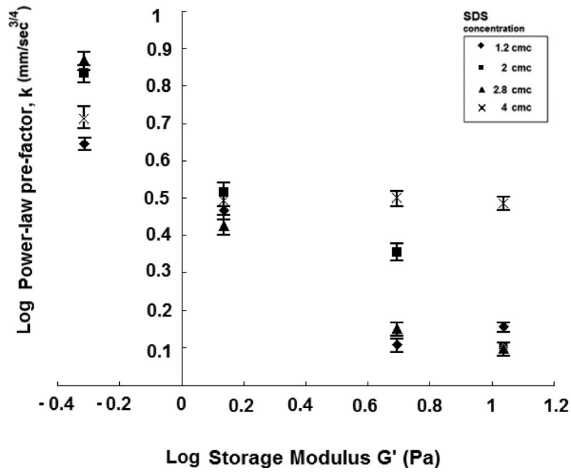

Figure 8. Dependence of log k on log G' for the spreading of SDS droplets. An increasing storage modulus corresponds to an increasing gel concentration.

droplet contacts the gel surface and no circular disk is formed initially, with the exception being concentrations higher than 0.10 wt % (in the cases of 8 cmc drops spread on 0.12 wt % gels and 1 cmc drops spread on 0.14 wt % gels, for instance). For lower surfactant concentrations, the pattern morphologies look comparatively less complicated, whereas increasing the surfactant concentration leads to more complex morphologies. For instance, the patterns that occur when droplets of very high surfactant concentration (between 6 cmc and 8 cmc) are spread on agar gels with concentrations near 0.04 wt % have arms with no well-defined edges, but ridges along the edges can be observed instead (Figure 11E,F). When the more concentrated droplets spread on much stronger gels (concentrations near 0.14 wt %), thin cracks emerge from the edges of the main cracks (Figure 11A,B). The formation of the latter can be a result of the relief of the surface-tension-induced stresses from new arms emanating from the existing ones because the crack formation is limited by the diameter of the Petri dish. Such behavior was not observed in the case of SDS.

dx.doi.org/10.1021/la205163n | *Langmuir* 2012, 28, 7197−7211

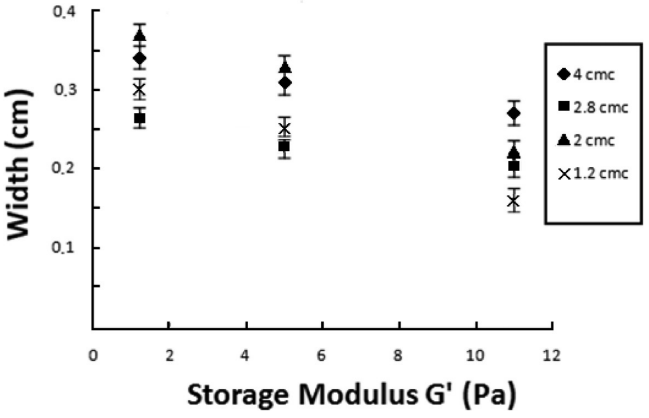

Figure 9. Dependence of the width of the pattern arms on the storage modulus of the agar gel. Each point represents the average of multiple runs. G' = 1.38 Pa corresponds to 0.08 wt % agar, G' = 5 Pa corresponds to 0.10 wt % agar, and G' = 11 Pa corresponds to 0.12 wt % agar.

Figure 12 shows a typical example of the spatiotemporal evolution of the patterns. Most patterns observed took less time to fully develop compared to the case of SDS, and the growth of the cracks is usually complete after 15−20 s. This difference manifests the superior spreading ability of Silwet L-77 and can probably be attributed to the fact that Silwet L-77 is more surface active than SDS.

Figure 13 shows that a majority of the values for the spreading exponent n of the power law $L(t) \approx kt^n$ for a starburst arm are close to $^3/_4$, with values near $^1/_2$ also observed. These findings are independent of surfactant and gel concentrations and suggest that the spreading is Marangoni-driven.

The superspreading behavior of Silwet L-77 is evident when the velocity of the evolution of the cracks is considered; this velocity for the spreading of Silwet L-77 is much higher than the velocity of SDS spreading, as suggested by a comparison between the values of log k in Figures 8 and 14. When Silwet L-77 is used on the same substrate, higher values of log k and k can be achieved.

The ability of Silwet L-77 to promote more rapid crack propagation speeds than SDS is illustrated in Figure 15, where dL/dt is plotted against time for Silwet L-77 and SDS droplets spreading on agar gel substrates of the same concentrations. The spreading rates associated with Silwet L-77 are consistently higher than those of SDS.

This finding becomes even more intriguing given that the concentrations of Silwet L-77 used in the experiment are much smaller than those of SDS because the cmc of Silwet L-77 is much smaller than the cmc of SDS. In other words, Silwet L-77 can promote extremely rapid spreading and cracking because even at concentrations smaller by an order of magnitude than those of SDS it can generate higher arm-formation and crack-propagation speeds. This can be explained by the fact that Silwet L-77 is more surface active than SDS and also by the significance of the adsorption of superspreading surfactants at the substrate (analyzed further in the Discussion section). Such rapid spreading rates can be tentative evidence for assuming that there is no accumulation of the superspreading surfactant at the contact line, and this can be achieved possibly by adsorption of the surfactant at the contact line and its subsequent diffusion away from this region, which reduces the surfactant concentration in relation to that upstream, sustaining the magnitude of the Marangoni stresses. Superspreading trisiloxane surfactants such as Silwet L-77 that are adsorbed at the air/liquid interface are more likely to transfer directly onto the substrate, compared to nonsuperspreading surfactants.[62] Figure 15 also demonstrates that crack propagation is faster on the surfaces of weaker gels but slower on stronger gels.

The increase in gel concentration seems to have an effect on the width of the arms, with the arms becoming thinner with increasing concentration (Figure 16), as in the case of SDS.

4. DISCUSSION

4.1. Spreading Exponent. The results shown in Figures 7 and 13 indicate that that the power-law scaling of the evolution of the length of a starburst arm varies from $L \approx t^{1/2}$ to $t^{0.85}$, with the majority of the spreading patterns being found to grow with time as $L \approx t^{3/4}$, independently of the gel concentration and the surfactant type and concentration. The crack length and growth rate reflect the spreading of the surfactant. The $t^{3/4}$ scaling is characteristic of Marangoni-driven spreading on thick films, suggesting that Marangoni stresses are dominant for the cases examined here. Daniels et al.[21] also found values close to $n = {}^3/_4$ for the spreading of PDMS and Triton X-305 on agar gels and in a geometry similar to that used in our experiments. It should be noted that the only surfactant used in the latter study was Triton X-305; therefore, it could be expected that there will be no agreement with the $t^{3/4}$ scaling prediction in the case of PDMS, which is not a surfactant. However, the patterns formed during the spreading of PDMS were also found to grow with time as $L \approx t^{3/4}$.[21] The roots of this phenomenon could be attributed to the fact that PDMS solutions can have a much lower surface tension than water, typically 20 mN/m,[21] giving rise to Marangoni stresses that could still play a role in the spreading process.

The same time dependence has been both theoretically predicted[78,79] and experimentally confirmed in the past, for instance, in a recent study by Berg[69] on the spreading of SDS and DTAB surfactants along the interface between thick layers of water and decane. It has also been confirmed in the case of oil and silicon oil spreading on water,[2,79−82] on surfactant solutions,[83] and on the surfactant-induced fracture of a particle raft.[18] All of the studies mentioned above considered spreading on viscous liquids, and it should be noted that the theoretical argument behind the $t^{3/4}$ scaling requires the assumption that the surface tension gradient is balanced by the viscous drag of the underlying fluid,[69] which is not applicable to solids.

The $t^{1/2}$ scale is characteristic of the diffusive spreading of surfactants or the spreading of surfactant from an infinite reservoir.[84] In the case of gels, Szabó et al.[10] and Kanenko et al.[11] report an $R \approx t^{1/2}$ scaling in the studies involving the spreading of different liquids on the surface of PAMS (2-acrylamido-2-methylpropanesulfonic acid) gels. More specifically, Kanenko et al.[11] found values of the spreading exponent for a polymer gel underlying layer of n = 0.45 and 0.3 for miscible and immiscible spreading liquids, respectively. It should be noted, however, in the latter studies that large Marangoni stresses are absent, and it is argued that the spreading on the surface of a highly concentrated gel is very similar to that on a solid surface; therefore, the assumption that takes into account the effect of the viscous drag of the underlying fluid is not applicable to solids. However, the gels that we examine in this study have very low concentrations and are largely composed of water; therefore, it is not appropriate to

dx.doi.org/10.1021/la205163n | Langmuir 2012, 28, 7197−7211

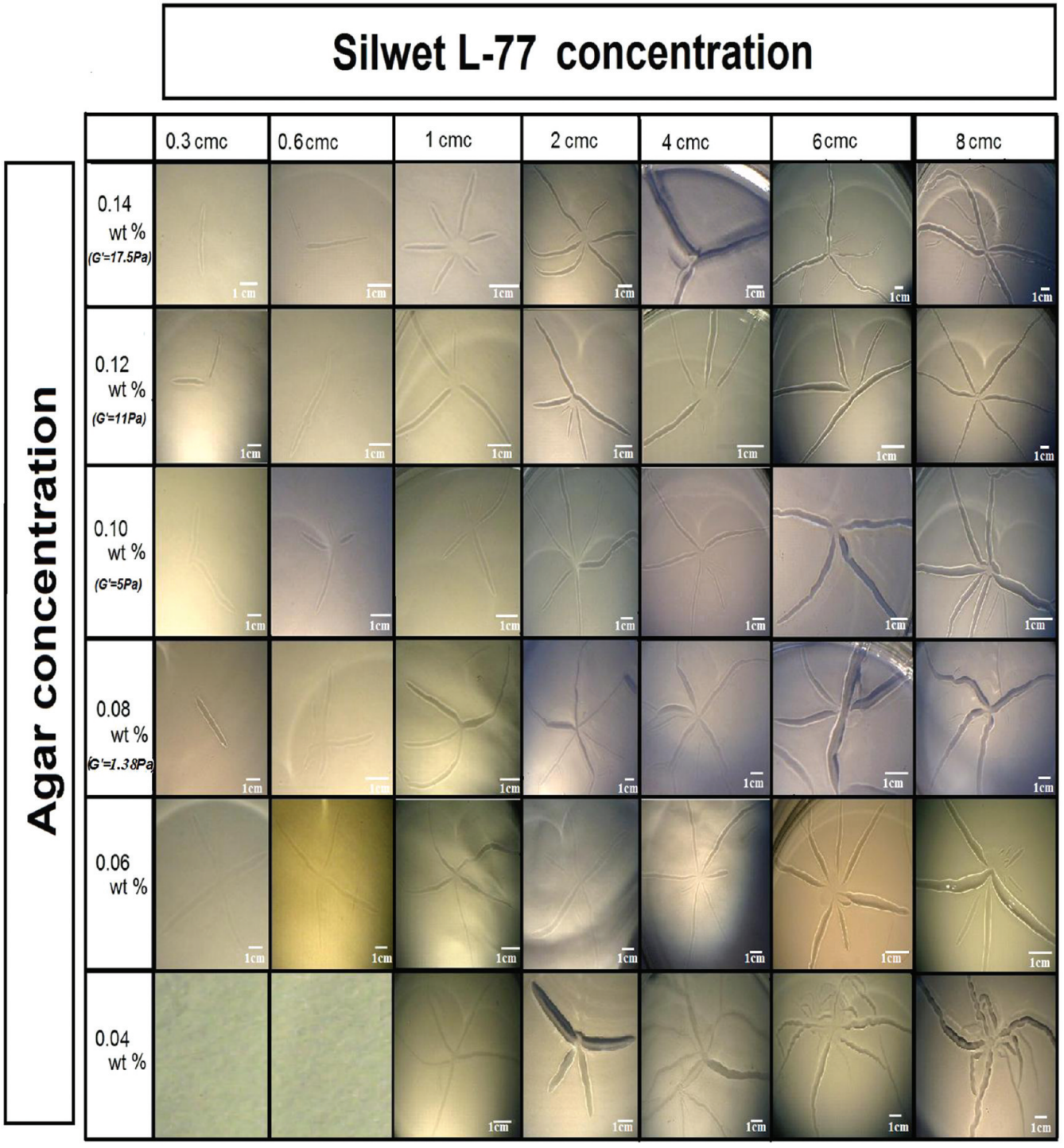

Figure 10. Pattern map showing fully developed patterns from Silwet L-77 droplets of different concentrations that have spread on approximately 4-mm-thick agar gel layers of varying concentrations.

characterize their behavior as dominantly solid-like, particularly on the molecular scale.

The fact that not all arms of the same pattern were shown to grow following the same scaling relationship can be explained by the high degree of local heterogeneities on the surface of a gel. These arise from the fact that a gel consists of heterogeneous populations of molecules that can have different physicochemical and hence mechanical properties.[85] Therefore, on a local level, concentration and surface tension gradients can arise between different regions of the same gel surface. Weaker gels can exhibit more heterogeneities than stronger gels.[86] In the surfactant-induced gel fracture studied here, concentration and surface tension gradients can affect the crack propagation phenomenon in terms of the size and the shape of the arms and in terms of the propagation velocities. The nonuniformities on the surface are also responsible for the fact that the starbursts are asymmetrical and that the patterns of the same starburst are not morphologically identical to each other. Furthermore, the conditions in a specific region of the gel surface can be different from those in a neighboring region. Therefore, the conditions

dx.doi.org/10.1021/la205163n | *Langmuir* 2012, 28, 7197−7211

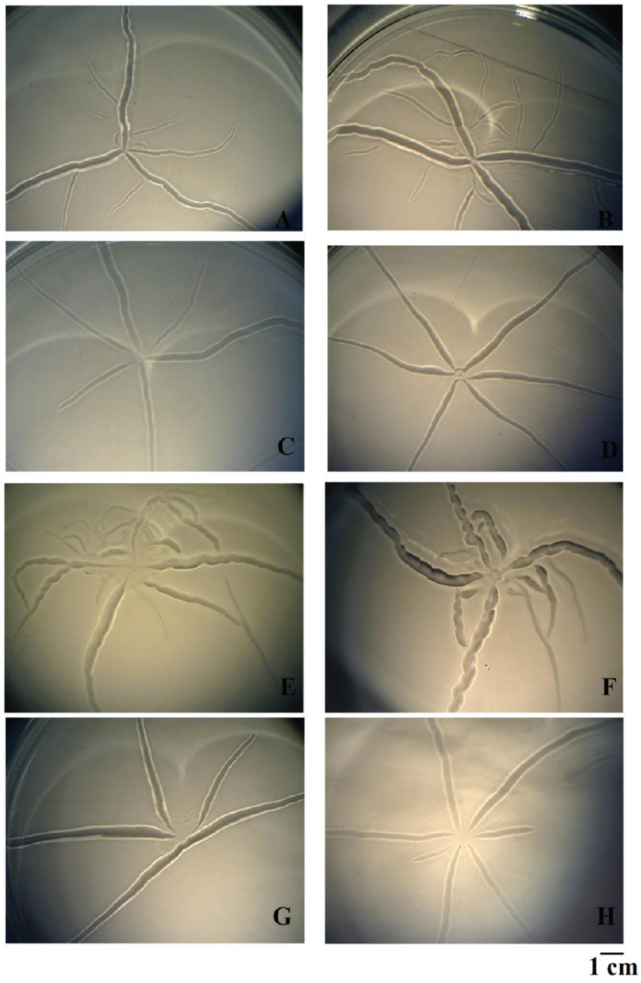

Figure 11. Close-up view of shadowgraph images of fully developed patterns after the spreading of (A) 6 cmc Silwet L-77 on 0.14 wt % agar, (B) 8 cmc Silwet L-77 on 0.14 wt % agar, (C) 2 cmc Silwet L-77 on 0.10 wt % agar, (D) 8 cmc Silwet L-77 on 0.12 wt % agar, (E) 6 cmc Silwet L-77 on 0.04 wt % agar, (F) 8 cmc Silwet L-77 on 0.04 wt % agar, (G) 6 cmc Silwet L-77 on 0.12 wt % agar, and (H) 4 cmc Silwet L-77 on 0.06 wt % agar.

for one potential arm may be different and more conducive to growth from those of another. In addition, as an arm grows it may shield and hinder the growth of a neighboring arm by making the conditions less conductive to growth (smaller concentration gradients, for instance). The large opportunity for discrepancies in the rheology of the gel can also increase the degree of local heterogeneities because even small disturbances in the gel surface during its preparation, storage, or use can change its rheological properties.

4.2. Mechanism: Initiation and Hindrance of Crack Growth. Given the dominant presence of Marangoni stresses in the SDS agar and Silwet L-77 -agar systems, it can be suggested that the formation of the starburst patterns is the result of the competition between those stresses and the gel strength and that the main driving force behind the cracking instability that manifests itself via the formation of these patterns is the surface tension gradients generated between the surfactant and the gel.

Whether a droplet spreads on a gel surface is thermodynamically determined by the spreading coefficient[87]

$$S = \sigma_g - \sigma_d - \sigma_{gd} \quad (4)$$

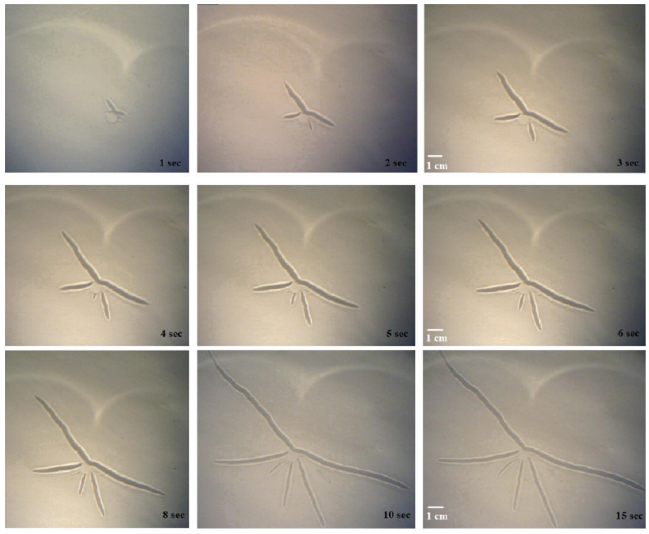

Figure 12. Spreading pattern evolution with time after the deposition of a 2 cmc Silwet L-77 droplet on a 0.12 wt % agar gel. After t = 15 s, the evolution is complete.

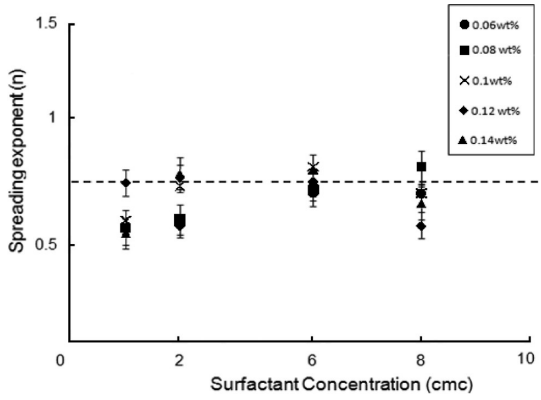

Figure 13. Variation of the spreading exponent with Silwet L-77 concentrations for spreading on agar gel layers of different concentrations. These points represent the average of the multiple runs. The dashed line is the theoretical value of $^3/_4$ that is characteristic of Marangoni-driven spreading on thick layers.[2,76,77]

with σ_g, σ_d, and σ_{gd} being the interfacial tensions for gel−air, droplet−air, and gel−droplet, respectively. The droplet will spread if $S \geq 0$. Under the assumption that σ_{gd} is negligible[20,21] because both the droplet and the gel are mainly composed of water, the spreading parameter is defined as $S \equiv \sigma_g - \sigma_d$. The crack-like patterns can be formed when the surface tension gradients are sufficiently large to generate Marangoni stresses strong enough to overcome the resistance of the rigidity of the gel and to form cracks on its surface. This explains the observation of a higher probability for cracks to occur in cases where the surfactant concentration is large and the gel concentration is small. Because the length scales along the direction of propagation are longer than those perpendicular to it, one expects the largest surface tension gradients to be in the latter direction. Hence, one also expects that this will lead to an unzipping of the gel in a manner perpendicular to the direction of the largest surface tension gradient, as shown in the schematic depicted in Figure 17. This mechanism highlights the width of the arms as an important parameter that can characterize this spreading instability.

dx.doi.org/10.1021/la205163n | Langmuir 2012, 28, 7197−7211

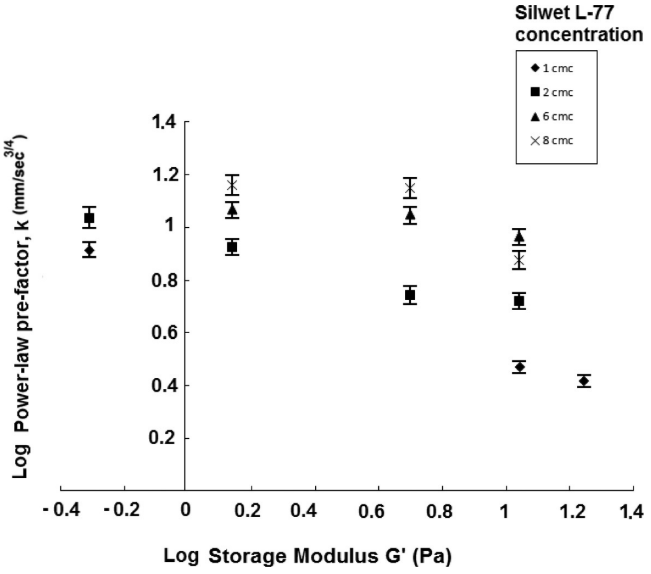

Figure 14. Dependence of log k on log G' for the spreading of Silwet L-77 droplets. An increasing storage modulus corresponds to an increasing gel concentration.

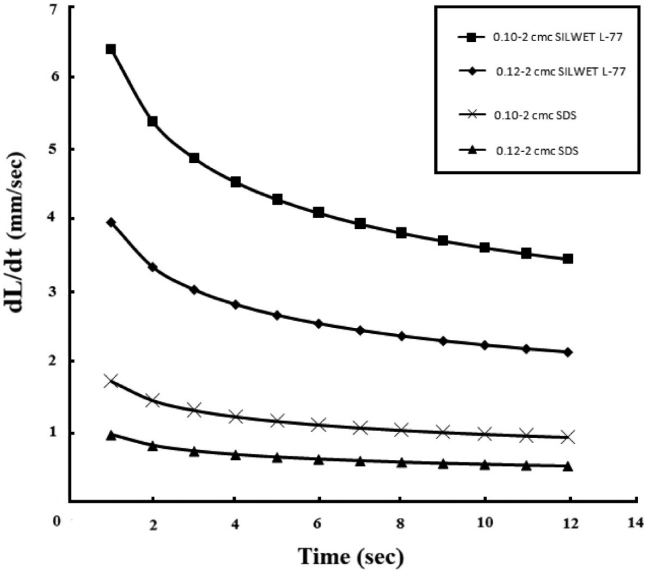

Figure 15. Comparison between the spreading rates of 2 cmc Silwet L-77 on 0.10 and 0.12 wt % agar gel and the spreading rates of 2 cmc SDS on the same substrates.

It is easier to visualize this assumed unzipping mechanism by creating a small artificial crack of known size on the surface of the gel with a needle and then depositing a droplet of surfactant inside the crack and measuring its increased width, as illustrated in Figure 18. The way that the crack opens during its propagation gives an impression of unzipping to the observer.

Because the width of the cracks can be associated with the storage modulus of the gel (Figures 9 and 16), a change in the width (Δw) together with the difference in surface tension can quantify a stress that can be compared to the storage modulus. Therefore, a crack-like arm will be formed on the surface of the gel if

$$\frac{S}{\Delta w} \geq G' \qquad (5)$$

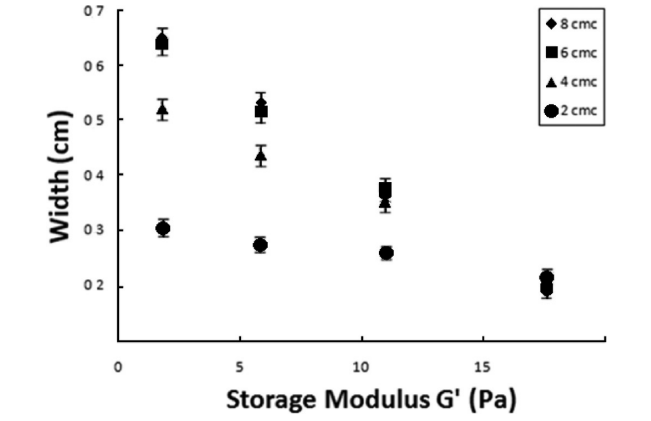

Figure 16. Dependence of the width of the pattern arms on the storage modulus of the agar gel. Each point represents the average of multiple runs. G' = 1.38 Pa corresponds to 0.08 wt % agar, G' = 5 Pa corresponds to 0.10 wt % agar, G' = 11 Pa corresponds to 0.12 wt % agar, and G' = 17.5 Pa corresponds to 0.14 wt % agar.

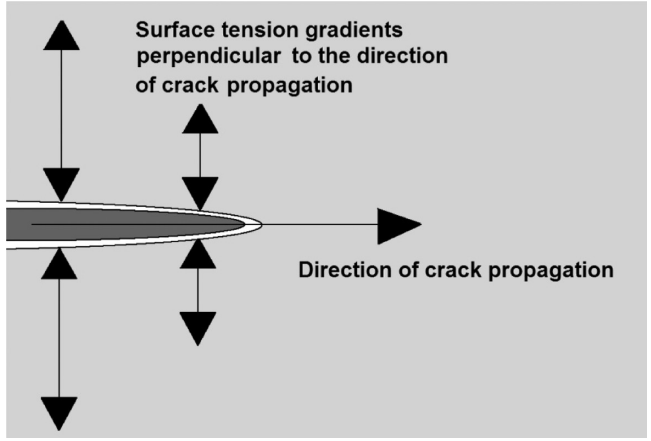

Figure 17. Unzipping of a crack perpendicular to the direction of surface tension gradients.

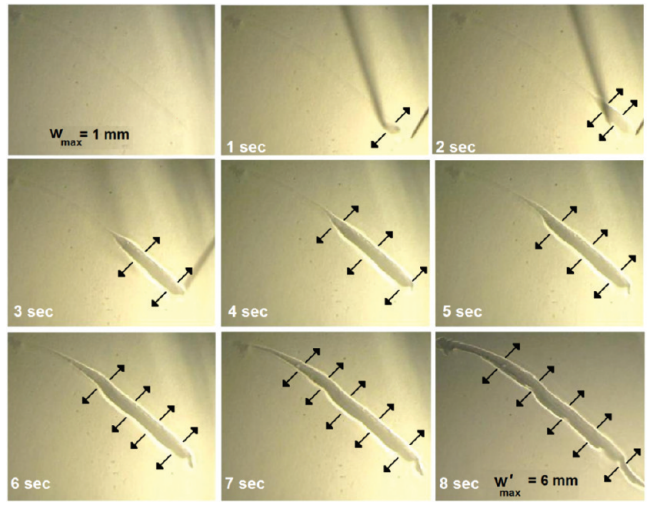

Figure 18. Artificial crack, 1 mm in width, created on the surface of a 0.10 wt % agar gel. Eight seconds after the deposition of a 6 cmc Silwet L-77 droplet the width of the crack increases to a maximum of approximately 6 mm. The directions of the arrows show how the crack unzips.

dx.doi.org/10.1021/la205163n | Langmuir 2012, 28, 7197−7211

Inequality 5 is similar to the one suggested by Daniels et al.[21] in characterizing the Marangoni instability and in associating it mainly with the number of arms that can form. Daniels et al.[21] found that the number of arms depends on the gel strength. In a recent study on the cracking of a jammed particle band formed by the introduction of a surfactant droplet into a monolayer of hydrophobic particles, the number of cracks was observed to depend on the initial packing fraction.[88] In our experiments, however, no clear trend that could connect changes in the gel and surfactant concentration to changes in the number of arms was identified, and the distribution of the number of arms was scattered fairly evenly across the range of cases studied. Therefore, the number-of-arms parameter is not taken into consideration in this study.

A comparison of $S/\Delta w$ against G' for all of the cases studied here is illustrated in Figures 19 and 20, where it is shown that

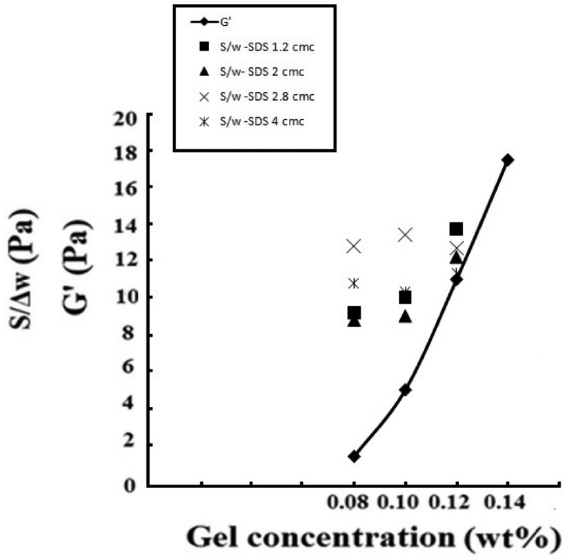

Figure 19. $S/\Delta w$ and G' against the agar gel concentration, with the SDS concentration varying parametrically. $S/\Delta w$ is consistently greater than G' wherever cracking patterns are observed.

inequality 5 is valid for both surfactants and within the limits of the surfactant and gel concentration where a pattern can be formed. For lower gel concentrations, $S/(\Delta w)$ is much greater than G', and this results in the formation of very wide arms, whereas for very high gel concentrations $S/(\Delta w)$ is greater than but very close to G', and this results in the formation of very narrow arms. A further concentration increase does not allow any arm formation. Thus, it may be possible using inequality 5 to get an estimate of the arms' width by dividing S by G', both of which are a priori measurable quantities.

For the agar gel concentrations where the cracks were observed, the gel is in an intermediate situation and can behave like both a solid and a liquid. For the high concentrations within these limits, the substrate starts to behave more like a solid, even though this behavior is not as dominant as at even higher concentration (where eventually there would be no crack formation). Therefore, the characteristics of spreading on both solid and liquid substrates can be attributed to this phenomenon, and the adsorption and diffusion of the surfactant can both participate in the spreading process.

The high crack propagation speeds (Figures 8 and 14) are indicative of very high Marangoni stresses that can promote

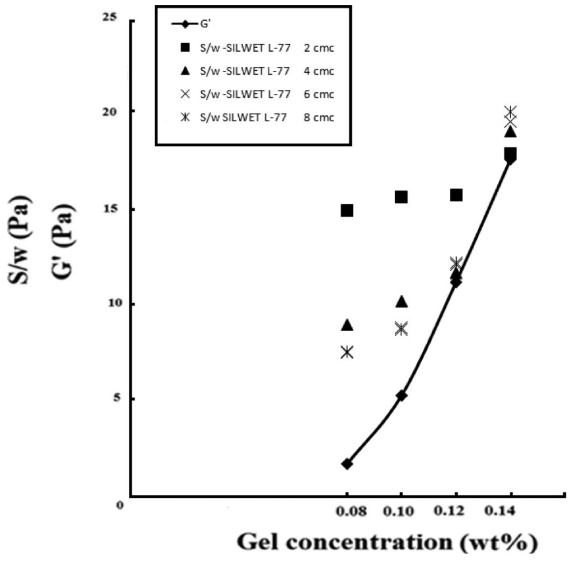

Figure 20. $S/\Delta w$ and G' against agar gel concentration, with te Silwet L-77 concentration varying parametrically. $S/\Delta w$ is consistently greater than G' wherever cracking patterns are observed.

very rapid arm growth. To get such high Marangoni stresses, especially at concentrations much higher than the cmc examined here, it is essential for the accumulation of the surfactant at the contact line to be prevented. This can be possible by the adsorption of the surfactant on the substrate, which induces high surface tension gradients and in turn generates high Marangoni stresses. For spreading on solids, the unique behavior of superspreaders has been associated with their ability to adsorb at the substrate. The adsorption of a surfactant at the substrate has been considered to be an important factor by researchers in the spreading process[56,63,71,89,90] and in other phenomena such as the autophobic effect.[91] Karapetsas et al.[63] suggests that a soluble superspreading surfactant can adsorb at the solid surface through two mechanisms: either the surfactant monomers that reside in the bulk can freely adsorb/desorb at the substrate, or the surfactant monomers in the liquid−air interface can adsorb/desorb directly at the substrate through the contact line.

For Silwet L-77, the ability to adsorb significantly at the substrate has been attributed to the intriguing T-shaped structure of the trisiloxane molecule and the large area of the hydrophobic trisiloxane group.[61,71,92] The structure of trisiloxane surfactants allows them to adsorb directly onto a solid surface when dissolved in an aqueous phase and to assemble into bilayers at the contact line. On the contrary, for a nonsuperspreading surfactant adsorbed at the air/liquid interface, it is less possible to transfer directly onto the surface of the underlying substrate, but it tends to accumulate in front of the contact line.[62] In addition, because a gel consists of a network of polymer chains, the adsorption of the surfactant on the liquid/gel interface could possibly occur in the form of an entanglement of the surfactant molecules with the polymer chains. In this case, the hydrophobic part of the surfactant molecule would be attached to the polymer chain and the hydrophilic part would be attached to the aqueous phase. Because of its T-shaped structure, a Silwet L-77 molecule would be more favorable to entangle in a polymer chain and to provide better packing, compared to an SDS molecule. To support the latter theory, however, more information on the

dx.doi.org/10.1021/la205163n | Langmuir 2012, 28, 7197−7211

molecular structure and the molecular dynamics of the materials involved here needs to be obtained because one has to investigate whether the sizes of the surfactant molecules and the polymer chains would allow such an entanglement.

It is also worth examining the relative strength of the Marangoni stresses with respect to other forces that might be present; the surface Peclet number Pe_s gives a measure of the relative strength of Marangoni stresses to surface diffusion transport, and it is defined as $Pe_s = SH_o/\mu D_s$, where S is the spreading coefficient or the surface tension between the surfactant and the gel, H_o and μ are the thickness and the viscosity of the underlying fluid, respectively, and D_s is the surface diffusivity. For all cases of SDS spreading studied, S varied from 22 to 35 mN/m, whereas for Silwet L-77 spreading, S varied from 36 to 47.5 mN/m. Therefore, Pe_s was found to be on the order of 10^8 for both surfactants, suggesting that Marangoni stresses dominate surface diffusive effects. The relative strength of Marangoni stresses with respect to bulk diffusion transport is given by the bulk Peclet number Pe_b defined as $Pe_b = (UH_o)/(D_b) = \varepsilon(SH_o/\mu D_b)$, where $\varepsilon = H_o/L_o$ is the aspect ratio of the developed crack and has to be much less than 1 for the lubrication approximation to hold in the theoretical studies on drop spreading. Here, L_o is the length of the developed crack, which can be of the order of 10^{-3} m when the cracks start to develop and then increases to the order of 10^{-2} m at later times. Therefore, for both surfactants ε is initially on the order of 1 and decreases thereafter; Pe_b is initially on the order of 10^8 and can decrease to the order of 10^6 when the developed cracks become longer, suggesting that Marangoni stresses once again dominate and that bulk diffusive transport can be more significant than surface diffusion.

For thick underlying films, Marangoni stresses and hydrostatic pressure are expected to act in opposition during the spreading process.[93,94] The Bond number, Bo, expresses the relationship between the two physical mechanisms and is defined as[93] $BO \equiv (\rho H_o^2 g)/S$, where ρ is the density of the underlying fluid and g is the gravitational acceleration. Bo is likely to achieve its greatest value for low surfactant concentrations on a thick substrate. For the spreading of SDS, Bo achieves values of between 4.6 and 7.2, whereas for the spreading of Silwet L-77 Bo achieves values of between 3.3 and 4. This suggests that gravitational forces play a significant role in the spreading of both surfactants on thick agar gel layers. However, in the case of Silwet L-77 they seem to be less significant than in the case of SDS.

A combination of different effects can be responsible for preventing the further growth of the arms. The relaxation of the surface tension gradients due to the accumulation of surfactant when the initial surfactant concentration is high, or at later times during the spreading of a surfactant of intermediate concentration is the most obvious one; at low surfactant concentrations, the surface tension gradients are not sufficiently large to give rise to pattern formation. At very large surfactant concentrations, surfactant might accumulate at the contact line, resulting in the reduction of surface tension gradients, or even in the generation of reverse Marangoni forces. At intermediate concentrations, large surface tension gradients can be generated and maintained, and the formation of the crack occurs. However, in this case, the surface tension gradients can relax with time, when the rate of surfactant transport near the contact line is higher than the rate of its removal. At this stage, significant gravitational forces can increase further.

As observed in Figures 4−6 and 10−12, all of the cracks have a central darker region surrounded by a slightly elevated brighter border that represents the contact line between the crack and the uncontaminated gel. This elevated region in the contact line can be linked to the thickening regions that can be created locally at the surfactant leading edge from the disturbance in the film height caused by Marangoni spreading on liquids.[33,34,47] It could also be considered to be the analogue of the raised rim that is observed during the surfactant superspreading on solids.[56,63,95] In the region very close to the contact line, the surfactant concentration is reduced by the adsorption of the surfactant. The high surface tension generated locally resists the deformation of the interface and allows the contact angle to retain high values, leading to the formation of this elevated rim.

The significance of gravitational forces highlighted by the high values of the Bond number has an effect on preventing the arms from propagating further on the surface of the gel. With time, gravitational effects increase while the surface tension gradients are relaxed. Gaver and Grotberg[93] suggested that, whenever hydrostatic forces overwhelm Marangoni stresses, a flow reversal effect can arise. This will move fluid from the thickened or elevated regions back to the thinning regions (cracks) of the substrate, diminishing the original substrate height disturbance.

5. CONCLUSIONS

Parametric experimental work that involves the spreading of SDS and Silwet L-77 surfactant solutions on the surfaces of agar layers was conducted in order to contribute to the fundamental understanding of the complex interactions between surfactants and underlying gels. The spreading of droplets of both surfactant types on approximately 4-mm-thick agar gel layers was found to be accompanied by the formation of cracking patterns that are similar morphologically to those observed by Daniels et al.[21] The typical pattern observed constitutes mainly crack-like projections emanating from the location where the surfactant droplet is deposited on the gel layer. These projections can be described as spreading arms with well-defined edges that grow to resemble asymmetrical starburst formations. It is evident that the patterns can be formed only inside a "window" of surfactant and gel concentrations, which represents an intermediate state of the gel where it has elements from both solid-like and liquid-like behavior.

There seems to be an agreement with the $t^{3/4}$ scaling prediction of the evolution of the length of the cracks, suggesting that Marangoni stresses are dominant during the spreading in all cases examined here. Gravitational forces also play a role in the process. The spreading of Silwet L-77 results in higher crack-propagation speeds, as reflected by the higher values of power-law prefactor k measured for Silwet L-77 compared to those found for the spreading of SDS. The rapid crack propagation promoted by Silwet L-77 is even more intriguing given the fact that in this study Silwet L-77 was used in much smaller quantities compared to SDS. Thus, the superspreading behavior of Silwet L-77 is evident. The existence of a mechanism where the basic feature is the unzipping of the gel in a manner perpendicular to the direction of the largest surface tension is suggested. This is indicated by the fact that the length scales along the direction of crack propagation are longer than those perpendicular to it, hence the surface tension gradient is expected to be larger in the latter case. Therefore, the width of the arms, which in fact is found to

decrease while the gel concentration and strength increase, plays an important role in the cracking process. It was observed that a crack is formed on the gel surface only when $S/(\Delta w) \geq G'$ and via this equality it may be possible to control the width of the cracks by changing S and G'. Further growth of the arms is prevented when the Marangoni stresses are initially weak because of the very high surfactant concentration, or when they relax with time when the rate of surfactant transport near the contact line becomes higher than the rate of its removal. In the same period of time, gravitational forces become more significant and flow reversal is possible. When the latter occurs, fluid is moved from the elevated regions back to the interior of the cracks, leveling the original height disturbance of the substrate. It is also possible for an arm to hinder the growth of another neighboring arm by making the conditions in the specific region of the gel surface less conductive to growth.

■ ASSOCIATED CONTENT

Supporting Information

Additional rheological data. The effect of gelation time on storage modulus for 0.14 wt % agar gels for measurements after 7 h, 28 h, and 18 days (T = 20 °C). Flow curves for 0.14 wt % agar gels. This material is available free of charge via the Internet at http://pubs.acs.org.

■ AUTHOR INFORMATION

Corresponding Author

*E-mail: o.matar@imperial.ac.uk.

Notes

The authors declare no competing financial interest.

■ ACKNOWLEDGMENTS

We are grateful to Prof. Karen E. Daniels (North Carolina State University), Prof. James Grotberg (University of Michigan) and Dr. Daryl Williams (Imperial College London) for their valuable comments and suggestions concerning the imaging setup and to the EPSRC for funding this project.

■ REFERENCES

(1) Landt, E.; Volmer, M. Spreading velocity of oil on H_2O. *Z. Phys. Chem.* **1926**, *122*, 398.

(2) Hoult, D. P. Oil spreading on the sea. *Annu. Rev. Fluid Mech.* **1972**, *4*, 341.

(3) Grotberg, J. B. Pulmonary flow and transport phenomena. *Annu. Rev. Fluid Mech.* **1994**, *26*, 529.

(4) Grotberg, J. B. Respiratory fluid mechanics and transport processes. *Annu. Rev. Biomed. Eng.* **2001**, *3*, 421.

(5) McCulley, J. P.; Shine, W. E. The lipid layer of tears: dependent on meibomian gland function. *Exp. Eye Res.* **2004**, *78*, 361.

(6) Weinstein, S. J.; Ruschak, K. J. Coating flows. *Annu. Rev. Fluid Mech.* **2004**, *36*, 53.

(7) Knoche, M; Tamura, H; Bukovac, J. Performance and stability of the organosilicone surfactant L-77: effect of pH, concentration, and temperature. *J. Agric. Food Chem.* **1991**, *39*, 2002.

(8) Lee, K. S.; Ivanova, N.; Starov, V. M.; Hilal, N; Dutschk, V. Kinetics of wetting and spreading by aqueous surfactant solutions. *Adv. Colloid Interface Sci.* **2008**, *144*, 54.

(9) Matar, O. K.; Craster, R. V. Dynamics of surfactant-assisted spreading. *Soft Matter.* **2009**, *5*, 3801.

(10) Szabó, D.; Akiyoshi, S.; Matsunaga, T.; Gong, J. P.; Osada, Y.; Zrínyi, M. Spreading of liquids on gel surfaces. *J. Chem. Phys.* **2000**, *113*, 18.

(11) Kanenko, D.; Gong, J. P.; Zrínyi, M.; Osada, Y. Kinetics of fluids spreading on viscolesastic substrates. *J. Polym. Sci., Part B: Polym. Phys.* **2005**, *43*, 562.

(12) Huang, Y.; Leobandung, W.; Foss, A.; Peppas, N. A. Molecular aspects of muco- and bioadhesion: tethered structures and site-specific surfaces. *J. Controlled Release* **2000**, *65*, 63.

(13) Khanvikar, K.; Donovan, M. D.; Flanagan, D. R. Drug transfer through mucus. *Adv. Drug Delivery Rev.* **2001**, *48*, 173.

(14) Halpern, D.; Jensen, O. E.; Grotberg, J. B. A theoretical study of the surfactant and liquid delivery into the lung. *J. Appl. Physiol.* **1998**, *85*, 333.

(15) Andersson, H.; van den Berg, A. Microfabrication and microfluids for tissue engineering: state of the art and future opportunities. *Lab Chip* **2004**, *4*, 98.

(16) Seright, R. S. Clean up of oil zones after a gel treatment. *SPE Prod. Oper.* **2006**, *May*, 237.

(17) Seright, R. S. Understanding the Rate of Clean Up for Oil Zones after a Gel Treatment. SPE 112976, presented at the SPE/DOE Improved Oil Recovery Symposium held in Tulsa, Oklahoma, 2008.

(18) Vella, D.; Kim, H. Y.; Aussillous, P.; Mahadevan, L. Dynamics of surfactant-driven fracture of particle rafts. *Phys. Rev. Lett.* **2006**, *96*, 178301.

(19) Tsapis, N.; Bennett, D.; Jackson, B.; Weitz, D. A.; Edwards, D. A. Trojan particles: large porous carriers of nanoparticles for drug delivery. *Proc. Natl. Acad. Sci. U.S.A.* **2002**, *99*, 12001.

(20) Daniels, K. E.; Mukhopadhyay, S.; Behringer, R. P. Starbusts and wispy drops: surfactants spreading on gels. *Chaos* **2005**, *15*, 041107.

(21) Daniels, K. E.; Mukhopadhyay, S.; Houseworth, P. J.; Behringer, R. P. Instabilities in droplets spreading on gels. *Phys. Rev. Lett.* **2007**, *99*, 124501.

(22) Marmur, A.; Lelah, M. D. The spreading of aqueous solutions on glass. *Chem. Eng. Commun.* **1981**, *13*, 133.

(23) Troian, S. M.; Wu, X. L.; Safran, S. A. Fingering instability in thin wetting films. *Phys. Rev. Lett.* **1989a**, *62*, 1496.

(24) Frank, B.; Garoff, S. Origins of the complex motion of advancing surfactant solutions. *Langmuir* **1995**, *11*, 87.

(25) Frank, B.; Garoff, S. Temporal and spatial development of surfactant self-assemblies controlling spreading of surfactant solutions. *Langmuir* **1995**, *11*, 4333.

(26) Frank, B.; Garoff, S. Surfactant self-assembly near contact lines: control of advancing surfactant solutions. *Colloids Surf., A* **1996**, *116*, 31.

(27) Bardon, S.; Cachile, M.; Cazabat, A. M.; Fanton, X.; Valignat, M. P.; Villette, S. Structure and dynamics of liquid films on solid surfaces. *Faraday Discuss.* **1996**, *104*, 307.

(28) Cachile, M.; Cazabat, A. M. Spontaneous spreading of surfactant solutions on hydrophilic surfaces: C_nE_m in ethylene and diethylene glycol. *Langmuir* **1999**, *15*, 1515.

(29) Cachile, M.; Cazabat, A. M.; Bardon, S.; Valignat, M. P.; Vandenbrouck, F. Spontaneous spreading of surfactant solutions on hydrophilic surfaces. *Colloids Surf., A* **1999**, *159*, 47.

(30) Cachile, M.; Schneemilch, M.; Hamraoui, A.; Cazabat, A. M. Films driven by surface tension gradients. *Adv. Colloid Interface Sci.* **2002**, *96*, 59.

(31) He, S.; Ketterson, J. B. Surfactant driven spreading of a liquid on a vertical surface. *Phys. Fluids A* **1995**, *7*, 2640.

(32) Fischer, B. J.; Darhuber, A. A.; Troian, S. M. Streamlets and branching dynamics in surfactant driven flows. *Phys. Fluids* **2001**, *13*, 9.

(33) Afsar-Siddiqui, A. B.; Luckham, P. F.; Matar, O. K. Unstable spreading of aqueous anionic surfactant solutions on liquid films. Part 1. Sparingly soluble surfactant. *Langmuir* **2003**, *19*, 696.

(34) Afsar-Siddiqui, A. B.; Luckham, P. F.; Matar, O. K. Unstable spreading of aqueous anionic surfactant solutions on liquid films. Part 2. Highly soluble surfactant. *Langmuir* **2003**, *19*, 703.

(35) Afsar-Siddiqui, A. B.; Luckham, P. F.; Matar, O. K. Dewetting behavior of aqueous cationic surfactant solutions on liquid films. *Langmuir* **2004**, *20*, 7575.

(36) Troian, S. M.; Wu, X. L.; Herbolzheimer, E.; Safran, S. A. Fingering Instability of a Spreading Drop. In *Phase Transitions in Soft*

Condensed Matter; Riste, T., Sherrington, D., Eds.;Plenum Press: New York, 1989.
(37) Troian, S. M.; Herbolzheimer, E.; Safran, S. A. Model for the fingering instability of spreading surfactant drops. *Phys. Rev. Lett.* **1990**, *65*, 333.
(38) Matar, O. K.; Troian, S. M. Dynamics and Stability of Surfactant Coated Thin Spreading Films. In *Dynamics in Small Confining Systems III*; Drake, J. M., Klafter, J., Kopleman, R., Ed.; Materials Research Society: Pittsburgh, PA, 1996; Vol. *464*, p 237.
(39) Matar, O. K.; Troian, S. M. Linear stability analysis of an insoluble surfactant monolayer spreading on a thin liquid film. *Phys. Fluids A* **1997**, *9*, 3645.
(40) Matar, O. K.; Troian, S. M. Growth of non-modal transient structures during the spreading of surfactant coated films. *Phys. Fluids A* **1998**, *10*, 1234.
(41) Matar, O. K.; Troian, S. M. Spreading of surfactant monolayer on a thin liquid film: onset and evolution of digitated structures. *Chaos.* **1999**, *9*, 141.
(42) Matar, O. K.; Troian, S. M. The development of transient fingering patterns during the spreading of surfactant coated films. *Phys. Fluids A* **1999**, *11*, 3232.
(43) Warner, M. R. E.; Craster, R. V.; Matar, O. K. Unstable van der Waals driven line rupture in Marangoni driven thin viscous films. *Phys. Fluids.* **2002**, *14*, 1642.
(44) Warner, M. R. E.; Craster, R. V.; Matar, O. K. Dewetting of ultrathin surfactant-covered films. *Phys. Fluids* **2002**, *14*, 4040.
(45) Warner, M. R. E.; Craster, R. V.; Matar, O. K. Fingering phenomena associated with insoluble surfactant spreading on thin liquid films. *J. Fluid Mech.* **2004**, *510*, 169.
(46) Warner, M. R. E.; Craster, R. V.; Matar, O. K. Fingering phenomena created by a soluble surfactant deposition on a thin liquid film. *Phys. Fluids.* **2004**, *16*, 2933.
(47) Edmonstone, B. D.; Craster, R. V.; Matar, O. K. Surfactant-induced fingering phenomena beyond the critical micelle concentration. *J. Fluid Mech.* **2006**, *564*, 105.
(48) Marangoni, C. G. M. Sul principio della viscosita superficiale dei liquidi stabilitato dal sig. j. plateau. *Nuovo Cimento* **1872**, *2*, 239.
(49) Levich, V. G. *Physicochemical Hydrodynamics*; Prentice-Hall: Englewood Cliffs, NJ; 1962.
(50) Edwards, D. A.; Brenner, H.; Wasan, D. T. *Interfacial Transport Processes and Rheology*. Butterworth-Heinemann: New York, 1991.
(51) Halverson, J. D.; Maldarelli, C.; Couzis, A.; Koplik, J. Wetting of hydrophobic substrates by nanodroplets of aqueous trisiloxane and alkyl polyethoxylate surfactant solutions. *Chem. Eng. Sci.* **2009**, *64*, 4657.
(52) Zhu, S.; Miller, W. G.; Scriven, L. E.; Davis, H. T. Superspreading of water-silicone surfactant on hydrophobic surfaces. *Colloids Surf., A* **1994**, *90*, 63.
(53) Stoebe, T.; Lin, Z.; Hill, R. M.; Ward, M. D.; Davis, H. T. Enhanced spreading of aqueous films containing ethoxylated alcohol surfactants on solid substrates. *Langmuir* **1997**, *13*, 7270.
(54) Hill, R. M. Superspreading. *Curr. Opin. Colloid Interface Sci.* **1998**, *3*, 247.
(55) Hill, R. M. Silicone surfactants-new developments. *Curr. Opin. Colloid Interface Sci.* **2002**, *7*, 255.
(56) Rafai, S.; Sarker, D.; Bergeron, V.; Meunier, J.; Bonn, D. Superspreading: aqueous surfactant drops spreading on hydrophobic surfaces. *Langmuir* **2002**, *18*, 10486.
(57) Nikolov, A. D.; Wasan, D. T.; Chengara, A.; Koczo, K.; Policello, C. A.; Kolossvany, I. Superspreading driven by Marangoni flow. *Adv. Colloid Interface Sci.* **2002**, *96*, 325.
(58) Chengara, A.; Nikolov, A.; Wasan, D. Surface tension gradient driven spreading of trisiloxane surfactant solution on hydrophobic solid. *Colloids Surf., A* **2002**, *206*, 31.
(59) Chengara, A.; Nikolov, A.; Wasan, D. Spreading of a water drop triggered by the surface tension gradient created by the localized addition of a surfactant. *Ind. Eng. Chem. Res.* **2007**, *46*, 2987.
(60) Ivanova, N.; Starov, V.; Johnson, D.; Hilal, N.; Rubio, R. Spreading of aqueous solutions of trisiloxanes and conventional surfactants over PTFE AF coated silicone wafers. *Langmuir* **2009**, *25*, 3564.
(61) Radulovic, J.; Sefiane, K.; Shanahan, M. E. R. Dynamics of trisiloxane wetting: effects of diffusion and surface hydrophobicity. *J. Phys. Chem. C* **2010**, *114*, 13620.
(62) Maldarelli, C. On the microhydrodynamics of superspreading. *J. Fluid Mech.* **2011**, *670*, 1.
(63) Karapetsas, G.; Craster, R. V.; Matar, O. K. On surfactant enhanced spreading and superspreading of liquid drops on solid surfaces. *J. Fluid Mech.* **2011**, *670*, 5.
(64) Mukerjee, P.; Mysels, K. J. *Critical Michelle Concentrations of Aqueous Surfactant Systems*; National Bureau of Standards, U.S. Department of Commerce; Washington DC, 1970.
(65) Chang, C. H.; Franses, E. I. Modified Langmuir-Hinshelwood kinetics for dynamic adsorption of surfactants at the air-water interface. *Colloids Surf., A* **1992**, *69*, 189.
(66) Birch, W. R.; Knewtson, M. A.; Garoff, S.; Suter, R. M. Structure of precursing thin films of an anionic surfactant on a silicon oxide/silicon surface. *Langmuir* **1995**, *11*, 48.
(67) Shen, A. Q.; Gleason, B.; McKinley, G.; Stone, H. A. Fiber coating with surfactant solutions. *Phys. Fluids* **2002**, *14*, 11.
(68) Berg, S.; Adelizzi, E. A.; Troian, S. M. Experimental study of entrainment and drainage flows in microscale soap films. *Langmuir* **2005**, *21*, 3867.
(69) Berg, S. Marangoni-driven spreading along liquid-liquid interfaces. *Phys. Fluids* **2009**, *21*, 032105.
(70) Lee, K. S.; Starov, V. M. Spreading of surfactant solutions over thin aqueous layers at low concentrations: influence of solubility. *J. Colloid Interface Sci.* **2009**, *329*, 361.
(71) Kumar, N.; Couzis, A.; Maldarelli, C. Measurement of the kinetic rate constants for the adsorption of superspreading trisiloxanes to an air/aqueous interface and the relevance of these measurements to the mechanism of superspreading. *J. Colloid Interface Sci.* **2003**, *267*, 272.
(72) Kiyohara, H.; Nagao, K.; Yana, K. Rapid screen for bacteria degrading water-insoluble, solid hydrocarbons on agar plates. *Appl. Environ. Microbiol.* **1982**, *43*, 454.
(73) Wolfe, A. J.; Berg, H. C. Migration of bacteria in semisolid agar. *Proc. Natl. Acad. Sci. U.S.A.* **1989**, *86*, 6973.
(74) Settles, G. S. *Schlieren and Shadowgraph Techniques: Visualizing Phenomena in Transparent Media*. Springer: New York, 2001.
(75) De Gennes, P. G. Wetting: statics and dynamics. *Rev. Mod. Phys.* **1985**, *57*, 827.
(76) Fay, J. A. The Spread of Oil Slicks on a Calm Sea. In *Oil on the Sea*; Hoult, D. P., Ed.; Plenum Press: New York, 1969.
(77) Jensen, O. E. The spreading of insoluble surfactant at the free surface of a deep fluid layer. *J. Fluid Mech.* **1995**, *293*, 349.
(78) Joos, P.; Pintens, J. Spreading kinetics of liquids on liquids. *J. Colloid Interface Sci.* **1977**, *60*, 507.
(79) Foda, M.; Cox, R. G. The spreading of thin liquid films on an water-air interface. *J. Fluid Mech.* **1980**, *101*, 33.
(80) Camp, D. W.; Berg, J. C. The spreading of oil on water in the surface tension regime. *J. Fluid Mech.* **1987**, *184*, 445.
(81) Dussaud, A. D.; Troian, S. M. Dynamics of spontaneous spreading with evaporation on a deep fluid layer. *Phys. Fluids.* **1998**, *10*, 23.
(82) Svitova, T.; Hill, R. M.; Radke, C. J. Adsorption layer structures and spreading behavior of aqueous dimethyldidodecylammonium bromide surfactant droplets over liquid hydrocarbon substrates. *Langmuir* **1999**, *15*, 7392.
(83) Bergeron, V.; Langevin, D. Monolayer spreading of polydimethylsiloxane oil on surfactant solutions. *Phys. Rev. Lett.* **1996**, *76*, 3152.
(84) Ahmad, J.; Hansen, R. S. A simple qualitative treatment of the spreading of monolayers on thin liquid films. *J. Colloid Interface Sci.* **1972**, *38*, 601.
(85) Lahaye, M.; Rochas, C. Chemical structure and physico-chemical properties of agar. *Hydrobiologia* **1991**, *221*, 137.

(86) Boyne, P.; Lechenault, F.; Daniels, K. E. *Analysis of Gel Heterogeneities on a Local Level*; presented at the 75th Annual APS Meeting, October 30−November 1, 2008.
(87) Harkins, W. D. *The Physics and Chemistry of Surface Films*.; Reinhold: New York, 1952.
(88) Bandi, M. M.; Tallinen, T.; Mahadevan, L. Shock-driven jamming and periodic fracture of particulate rafts. *Eur. Phys. Lett.* **2011**, *96*, 36008.
(89) Clay, M. A.; Miksis, M. J. Effects of surfactant on droplet spreading. *Phys. Fluids.* **2004**, *16*, 3070.
(90) Kim, H.-Y.; Qin, Y.; Fichthorn, K. A. Molecular dynamics simulation of nanodroplet spreading enhanced by linear surfactants. *J. Chem. Phys.* **2006**, *125*, 174708.
(91) Craster, R. V.; Matar, O. K. On autophobing in surfactant-driven thin films. *Langmuir* **2007**, *23*, 2588.
(92) Ananthapadmanabhan, K. P.; Goddard, E. D.; Chandar, P. A study of the solution, interfacial and wetting properties of silicone surfactants. *Colloids Surf., A* **1990**, *44*, 281.
(93) Gaver, D. P.; Grotberg, J. B. Droplet spreading on a thin viscous film. *J. Fluid Mech.* **1990**, *213*, 127.
(94) Gaver, D. P.; Grotberg, J. B. The dynamics of a localized surfactant on a thin film. *J. Fluid Mech.* **1992**, *235*, 399.
(95) Beacham, D. R.; Matar, O. K.; Craster, R. V. Surfactant-enhanced rapid spreading of drops on solid surfaces. *Langmuir* **2009**, *25*, 14174.